


Hydrogen concentration-induced stresses in an environmental TEMMatthew Connolly¹,* Veruska Malavé, and May L. Martin¹*National Institute of Standards and Technology, 325 Broadway, Boulder, Colorado 80305, USA* (Received 13 January 2022; accepted 29 March 2022; published 25 April 2022)

The hydrogen-enhanced localized plasticity (HELP) mechanism is a leading candidate among proposed hydrogen embrittlement (HE) mechanisms. Transmission electron microscopy (TEM) measurements of an increased dislocation mobility on exposure to hydrogen have provided the most direct evidence for the HELP mechanism. However, it has been hypothesized that the observed dislocation behavior is not a consequence of the interaction between hydrogen atoms and dislocations but a systematic error due to the nature of *in situ* TEM. Specifically, the electron beam in TEM microscopes can dissociate hydrogen, leading to a hydrogen fugacity much greater than the applied pressure. Such high fugacity will generate a large concentration gradient between the surface and interior of a TEM sample. It has been proposed that the observed dislocation mobility is due only to stresses arising from this concentration gradient rather than an effect of the interaction with hydrogen. Here we calculate the expected stresses for H/Fe and H/Ni systems fugacities expected in an *in situ* TEM. We show the stresses to be an order of magnitude too low to impact dislocation mobility in the H/Fe system, and that the concentration gradient-induced stresses dissipate quickly in both H/Fe and H/Ni systems—well before observation by TEM would occur.

DOI: [10.1103/PhysRevMaterials.6.L040601](https://doi.org/10.1103/PhysRevMaterials.6.L040601)

Hydrogen-enhanced localized plasticity (HELP) is a model of hydrogen embrittlement (HE) whereby hydrogen assists deformation, local to areas of high hydrogen concentration, which leads to the appearance of macroscopically brittle fracture [1]. The HELP-assisted deformation is facilitated by the formation of an atmosphere of hydrogen around dislocation stress fields, which reduces dislocation-dislocation interaction and accelerates dislocation motion. Although this concept was first formulated in 1972 [2], direct evidence of hydrogen-enhanced dislocation motion was not shown until 1983 [3] in iron. Later studies confirmed a similar effect in aluminum and aluminum alloys, nickel, steels, and titanium and titanium alloys [4–6].

The direct evidence for a hydrogen effect on dislocation mobility came in the form of *in situ* transmission electron microscopy (TEM) observations of dislocation motion before and after small partial pressures of hydrogen were introduced to the TEM environmental chamber. The first application of this technique determined an increase in dislocation velocity in iron through a frame-by-frame analysis after the introduction of hydrogen while the total specimen displacement was held fixed. The dislocation velocity was determined to be proportional to hydrogen pressure with a fivefold increase in dislocation velocity at a hydrogen pressure of 33 kPa [3] compared with in vacuum. Subsequently, dislocation activity was observed by TEM near a crack in two aluminum alloys. Both dislocation mobility and crack propagation rate were observed to increase in the presence of, at most, 13 kPa hydrogen.

Although the TEM-based evidence for the HELP mechanism has been observed in a wide range of material classes,

some doubt has been expressed that the dislocation motion is a result of hydrogen-dislocation interactions rather than a systematic effect of the experimental setup or sample preparation. For example, it was suggested by Oriani that the dislocation mobility was an effect of high hydrogen fugacities generated by the electron beam [7]:

... “because the very high hydrogen fugacity produced by the electron beam dissociating and ionizing the hydrogen can generate large mechanical stresses and hence large dislocation densities”.

Further, in a review of computational studies of HE, Tehrani and Curtin [8] suggested that a reason that computational work [9] did not reproduce experimental results, in addition to model size-limitation determined differences in geometry, could be this:

“One aspect of TEM studies is that the samples have a complex shape and nonuniform thickness. When charged with H, the TEM sample will then deform inhomogeneously, generating resolved shear stresses throughout the sample. These resolved shear stresses could act to push the pile-up dislocations closer together (with the lead dislocation being pinned in all cases by some unknown obstacle), and these stresses would be relieved when the H atmosphere is removed. However, such stresses are expected to be small in Al, which absorbs only small amounts of H. Thus, the TEM observations could possibly be due to such an extrinsic aspect of the experiment, and be general across the full spectrum of H-absorbing materials, but the issue remains open”.

In light of the uncertainty surrounding the TEM-based evidence for HELP, it is critical to investigate the magnitude of the generated stresses. There are three aspects of the argument to investigate: First, that the electron beam ionizes and dissociates the hydrogen in the environmental chamber,

*matthew.connolly@nist.gov

causing an increase in near-sample hydrogen fugacity beyond that measured by the pressure gauge on the environmental chamber; second, that such high fugacity leads to a high concentration of hydrogen near the surface of the sample; and finally, that this high concentration leads to stresses on the thin foil (thickness on the order of 100 nm) which are sufficiently high to impact dislocation mobility and pileup.

In a typical TEM experiment, a low partial pressure of H_2 (less than 40 kPa) was introduced into the TEM environmental chamber after the sample had been strained to generate mobile dislocations, in vacuum. The samples were necessarily thin, less than 200 nm, in order to be transparent to electrons. Electron beams were typically produced with accelerating voltages of 300 or 400 kV. Identical experiments using an inert gas (e.g., He) were typically used as controls, and reported dislocation mobility measurements were given in terms of ratios with respect to the inert gas measurements. That an electron beam with energies on the order of hundreds of kV can dissociate H_2 molecules in a gas, generating a high fugacity gas of H atoms, is generally well accepted. High hydrogen fugacity in environmental TEM studies was first noted by Oriani [7] and addressed later in Ref. [10], where lower and upper bounds on the hydrogen fugacity generated during environmental TEM measurements were determined based on the formation of blisters during an *in situ* TEM measurement in an $AlZn_{5.5}Mg_{2.5}$ alloy. A lower bound on the fugacity of approximately 40 MPa was determined from the curvature and surface tension of the observed blisters. An upper bound of the fugacity was determined by noting that yielding of the aluminum alloy was not observed, limiting the fugacity below that which would produce yielding approximately 750 MPa. Therefore there is experimental support that the electron beam increases the hydrogen fugacity by three to four orders of magnitude above the set pressure of the environmental chamber. The increase in fugacity is due to the interaction between the electron beam and the hydrogen gas and is therefore independent of the metal sample. In the following assessment of the second and third aspects of the argument, we will assume a worst-case scenario in which the hydrogen fugacity increases to 750 MPa during an *in situ* TEM experiment.

The second aspect of the argument is that the 750 MPa fugacity will lead to a high concentration of hydrogen at the surface of the sample. This aspect of the argument is certainly true. At a fugacity of 750 MPa, chemisorption of hydrogen will lead to a complete monolayer coverage on the metal's surface, a process which will take on the order of seconds [11]. However, a high concentration of hydrogen at the surface does not by itself generate stresses in the material. Rather, it is a concentration gradient that is required. While hydrogen from the gas phase is chemisorbing to the metal surface, some hydrogen will begin diffusing through the bulk metal, reducing the concentration gradient and equilibrating the stress. Nonetheless, in order to determine the highest possible concentration gradient induced stress achievable in a TEM experiment, we will work under the assumption that our initial state is one in which sufficient time has passed such that the near-surface concentration has reached a maximum, yet the hydrogen has not yet begun to diffuse into the bulk metal.

The third aspect of the argument is that the high hydrogen fugacity and subsequent increase in hydrogen concentration leads to sufficiently high stresses to affect dislocation motion. When Oriani initially proposed this concept he cited calculations by Li [12], which considered concentration-gradient-induced stresses in flat, uniform geometries. We will therefore first follow this reasoning through and calculate the magnitude of the stress from the work of Ref. [12]. Under the assumptions described above and under ideal sample preparation, TEM samples are thin foils having a fixed amount of solute deposited initially on the surfaces. A diagram of the thin foil sample and orientation are shown in Fig. 1(a). The H_2 gas, dissociated by the electron beam, acts as a constant supply of hydrogen and maintains a constant surface concentration. The H_2 gas is chemisorbed on the edges of the sample at $x = \pm a$, and the concentration of hydrogen in the sample varies only as a function of x and time t as the hydrogen diffuses through the bulk. At $t = 0$ the concentration is zero everywhere in the sample except at the surface, where the concentration is C_s . From Ref. [12], if the diffusivity is D and $p_n \equiv (2n + 1)\pi/2$, the concentration distribution C (moles/cm³) at time t is

$$\frac{C(x)}{C_s} = 1 - 2 \sum_{n=0}^{\infty} \frac{(-1)^n}{p_n} \cos \frac{p_n x}{a} \exp - \frac{p_n^2 D t}{a^2}. \quad (1)$$

The stress distribution is given by:

$$\begin{aligned} \sigma_{yy} &= \sigma_{zz} \\ &= \frac{2\bar{v}C_s E}{3(1-\nu)} \sum_{n=0}^{\infty} \frac{(-1)^n}{p_n} \left[\cos \frac{p_n x}{a} - \frac{1}{p_n} \right] \\ &\quad \times \exp \left(- \frac{p_n^2 D t}{a^2} \right), \end{aligned} \quad (2)$$

where \bar{v} is the partial molar volume of solute (cm³/mole), E is Young's modulus, and ν is Poisson's ratio. Table I shows the constants assumed for Fe and Ni.

The initial concentration can be determined from Sievert's Law,

$$C_s = K f^{1/2} \quad (3)$$

and assuming a fugacity f of H_2 of 750 MPa, where K is the solubility of hydrogen. For Fe, the solubility can be on the order of 3 ppm/MPa^{1/2} [13]. For Ni, the solubility is on the order of 24.5 ppm/MPa^{1/2} [14].

Figure 1(b) shows the diffusion-induced stress as a function of position for a range of times from 1 to 1000 ns for a 200-nm-thick foil of Fe and from 1 to 1000 ms for an identical foil of Ni. Because the diffusivity of hydrogen in Fe is quite high (10^{-4} cm²/s), the concentration equilibrates rapidly and the concentration gradient-induced stress diminishes after 1000 ns. Even in Ni, where the H diffusivity is several orders of magnitude lower (10^{-9} cm²/s), equilibrium occurs within 1 s. In the first instant after hydrogen is introduced, the concentration gradient-induced stresses are highest near the surface of the sample. The stresses are compressive near the surface and tensile in the interior. Significantly larger stresses arise in Ni compared with Fe because the solubility of hydrogen is higher in Ni. The maximum hydrogen concentration-induced stresses in Ni and Fe are well

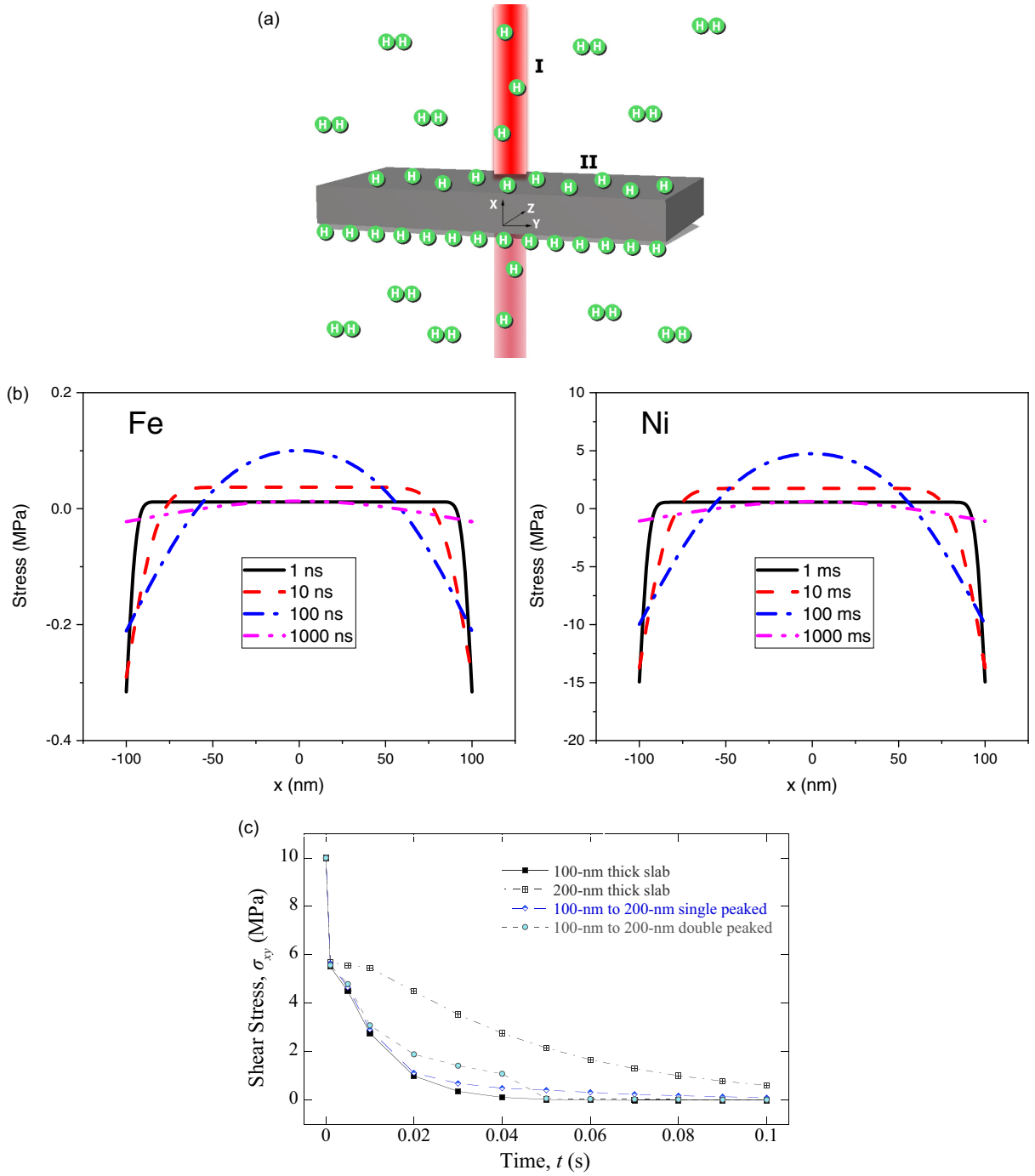


FIG. 1. (a) Schematic of the TEM experiment in an environmental chamber. The electron beam (red) dissociates H₂ molecules, (I), which increases the fugacity of H gas by orders of magnitude. H atoms chemisorb on the surface, (II), leading to a concentration gradient between the surface of the TEM sample and the interior. (b) The concentration gradient leads to mechanical stresses, which decay as H moves toward the sample’s interior. (c) The maximum shear stresses in a Ni sample are insufficient to generate dislocations, and dissipate within 0.1 seconds.

TABLE I. Physical constants assumed for the calculations of hydrogen-induced stresses in Fe and Ni.

	\bar{v} (cm ³ /mole)	E (GPa)	ν	D (cm ² /sec)	K (ppm/MPa ^{1/2})
Fe	2.66	210	0.33	10 ⁻⁴	3
Ni	1.70	190	0.305	10 ⁻⁹	24.5

below yield stress. However, the stress required to move an existing dislocation is the Peierls stress. In Fe, the Peierls stress for the $\{101\}\langle 11\bar{1}\rangle$ glide system is 2.7 MPa; in Ni, the Peierls stress for the $\{111\}\langle 10\bar{1}\rangle$ glide system is 3.1 MPa [15]. Clearly the hydrogen concentration-induced stresses in the Fe system are, by an order of magnitude, too low to move even the easiest glide systems. The stresses in Ni may, however, be sufficient to move dislocations based on the Peierls stress. However, for the flat sample geometry considered here so far and in Oriani’s original argument, with a large in-plane size compared with the through-thickness, the shear components of these stresses are all zero. Resolved shear stresses are necessary for causing dislocation movement, so the hydrogen concentration-induced stresses in a flat sample are not capable of moving dislocations.

As mentioned in Tehranchi and Curtin, TEM sample preparation leads to samples with nonuniform thickness, which may give rise to resolved shear stresses. We can calculate the stress under a worst-case scenario using a slanted geometry instead of a flat slab. Analytical solutions to the hydrogen concentration-induced stresses in a geometry with nonuniform thickness are not available, so finite element (FE) calculations were utilized to solve the mass transport equations, and the stress was determined using a linear elastic model with chemical strains. Transport of the hydrogen was assumed to be Fickian in the FE models. Full details of the FE calculations can be found in the Supplemental Material [16]. Because the stresses in Fe were shown to be an order of magnitude too low to affect dislocation motion, the FE calculations are only shown for the H/Ni system.

Figure 1(c) shows the maximum shear stresses determined in the FE calculations for a 100-nm-thick slab, a 200-nm-thick slab, a sample with 100 nm thickness at the edges with increased thickness toward the center to a maximum thickness of 200 nm (“singly-peaked”), and another sample with two peaks of the same size (“doubly peaked”) as a function of time. The FE calculations confirm zero shear stresses in the middle of the finite flat slab geometry. Near the edges of the sample, hydrogen concentration-induced shear stresses of approximately 6 MPa at 1 ms after exposure are observed; these stresses diminish within 100 ms. However, these shear stresses are highly local to the edges and would therefore only affect the ends of the dislocations as they approach the sample surface. In both the “singly peaked” and “doubly peaked” geometries, shear stresses of approximately 10 MPa are generated within the first 10 ms and dissipate around 100 ms after exposure. Because this stress is larger than the Peierls stress, it may be sufficient to affect dislocation motion provided that the glide plane is oriented in a way for a sufficient level of resolved shear stress. However, the shear stresses that are generated are dissipated when the H concentration reaches equilibrium (≈ 0.1 s), not when the H atmosphere is removed. Therefore, any effect observed after this relaxation time must be due to effects other than diffusion-induced stresses.

It should be noted that Ref. [12] pointed to seven cases of dislocation motion occurring during diffusion:

“Chemical stresses developed during diffusion can cause dislocation generation which may be desirable for surface hardening but not for electronic devices. Some examples of the studies of dislocations generated during diffusion are as

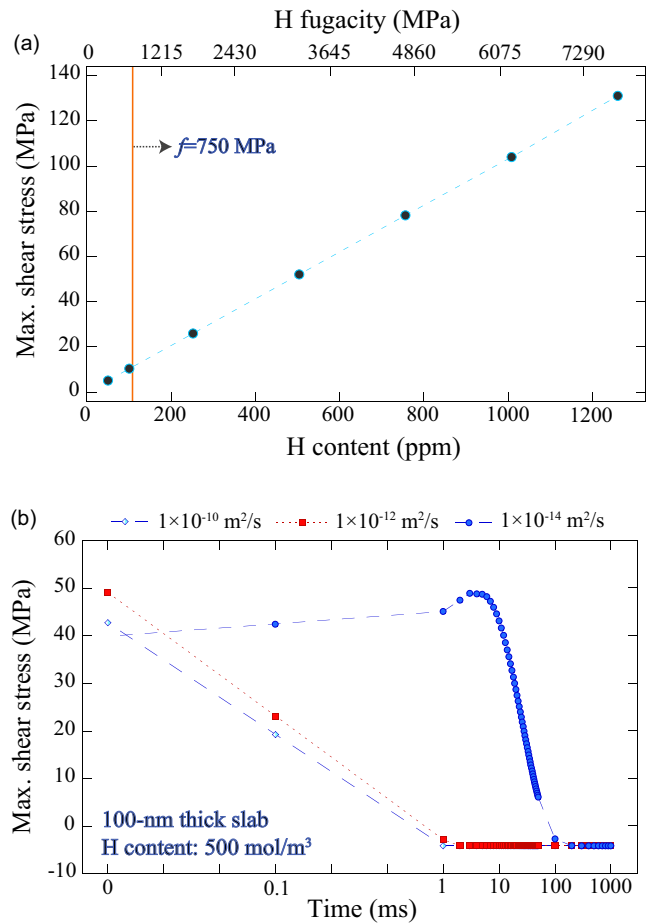


FIG. 2. (a) Maximum shear stress as a function of hydrogen fugacity. The upper bound of hydrogen fugacity is 750 MPa is shown by a dashed line. (b) Maximum shear stress as a function of time for a range of hydrogen diffusion coefficients. Even with a hydrogen diffusion 5 orders of magnitude slower than expected, any dislocation motion caused by hydrogen-induced stresses would dissipate within one second—while reported TEM measurements occur over minutes.

follows: Ayres and Winchel [17,18] measured dislocation density as a function of depth after diffusion of Zn into Cu. Boah and Winchel [19] studied dislocation configurations developed during carburization of Ni. Mozzi and Lavine [20] used x-ray rocking curves to study the damage induced by diffusion of Zn in InSb diodes. Sukhodreva and Cheryukanova [21] observed the formation of dislocations in Ge during the diffusion of As. Schwuttke and Queisser [22] applied x-ray microscopy to observe dislocations generated after diffusion of Ga, B, and P in Si. Miller *et al.* [23] used electron microscopy and other techniques to observe dislocations in Si after B diffusion. Washburn *et al.* [24] observed edge dislocation cross grids after P diffusion into Si”.

Note that we have altered the citation numbers in the above quote to reflect the citation numbers in this letter. One glaring difference between these seven observations of diffusion-induced dislocation movement and hydrogen-induced dislocation movement is the size of the solute, which is near the atomic size of the solvent in each of the seven cases. However, the most important difference between the

cases above is the concentration of solute, which in each example is on the order of percentage, whereas in the H in Ni or Fe case the concentration is on the order of one to hundreds of ppm. Armacanqui and Oriani [25] did observe dislocation motion in BCC Fe after charging with H; however, this was under severe electrochemical charging that led to a hydrogen concentration of 11%, several orders of magnitude higher than can be reached under the fugacity generated in an environmental TEM.

To illustrate just how severe the fugacity conditions would need to be to generate large enough stresses to affect the TEM measurements, we have calculated the maximum shear stresses induced as a function of hydrogen fugacity and show the results in Figure 2(a). The maximum shear stresses increase linearly with hydrogen fugacity; however, using an upper bound on hydrogen fugacity of 750 MPa, the maximum shear stresses are quite low. To illustrate just how slow hydrogen would need to move for any stress effect to be observed on the timescale of the TEM measurements used in support of the HELP mechanism, we show the maximum shear stress

dissipation as a function of time for a range of diffusion coefficients in Figure 2(b). Even if the hydrogen somehow were slowed to a diffusion coefficient of 10^{-14} m²/s—a full five orders of magnitude slower than expect for H in Ni—the stresses are equilibrated within 1 s.

In summary, even under the highest estimations of hydrogen fugacities, hydrogen concentration gradient-induced stresses are not sufficient to impact the observation of dislocation mobility in a typical TEM experiment on a H/Fe system. The shear stresses that are generated in the H/Ni system dissipate well before observation by TEM. Therefore claims that the dissociation of H₂ gas by the electron beam give rise to systematic errors in TEM observations related to the HELP mechanism are not supported.

Thanks to Roselyn Adams for the artwork presented in this Letter. The authors declare that they have no known competing financial interests or personal relationships that could have appeared to influence the work reported in this paper.

-
- [1] M. L. Martin, M. Dadfarnia, A. Nagao, S. Wang, and P. Sofronis, Enumeration of the hydrogen-enhanced localized plasticity mechanism for hydrogen embrittlement in structural materials, *Acta Mater.* **165**, 734 (2019).
 - [2] C. Beachem, A new model for hydrogen-assisted cracking (hydrogen “embrittlement”), *Metall. Mater. Trans. B* **3**, 441 (1972).
 - [3] T. Tabata and H. Birnbaum, Direct observations of the effect of hydrogen on the behavior of dislocations in iron, *Scr. Metall.* **17**, 947 (1983).
 - [4] P. Ferreira, I. Robertson, and H. Birnbaum, Hydrogen effects on the character of dislocations in high-purity aluminum, *Acta Mater.* **47**, 2991 (1999).
 - [5] P. Ferreira, I. Robertson, and H. Birnbaum, Hydrogen effects on the interaction between dislocations, *Acta Mater.* **46**, 1749 (1998).
 - [6] D. Teter, I. Robertson, and H. Birnbaum, The effects of hydrogen on the deformation and fracture of β -titanium, *Acta Mater.* **49**, 4313 (2001).
 - [7] R. Oriani, Whitney award lecture — 1987: Hydrogen — the versatile embrittler, *Corrosion* **43**, 390 (1987).
 - [8] A. Tehranchi and W. A. Curtin, The role of atomistic simulations in probing hydrogen effects on plasticity and embrittlement in metals, *Eng. Fract. Mech.*, **216** 106502 (2019).
 - [9] J. Song and W. Curtin, Mechanisms of hydrogen-enhanced localized plasticity: an atomistic study using α -Fe as a model system, *Acta Mater.* **68**, 61 (2014).
 - [10] G. Bond, I. Robertson, and H. Birnbaum, On the determination of the hydrogen fugacity in an environmental cell tem facility, *Scr. Metall.* **20**, 653 (1986).
 - [11] M. Connolly, M. Martin, R. Amaro, A. Slifka, and E. Drexler, Hydrogen isotope effect on the embrittlement and fatigue crack growth of steel, *Mater. Sci. Eng., A* **753**, 331 (2019).
 - [12] J. C.-M. Li, Physical chemistry of some microstructural phenomena, *Metall. Trans. A* **9**, 1353 (1978).
 - [13] J. Woodtli and R. Kieselbach, Damage due to hydrogen embrittlement and stress corrosion cracking, *Eng. Fail. Anal.* **7**, 427 (2000).
 - [14] Y. Ebisuzaki, W. Kass, and M. O’Keeffe, Diffusion and solubility of hydrogen in single crystals of nickel and nickel-vanadium alloy, *J. Chem. Phys.* **46**, 1378 (1967).
 - [15] S. Boffi, G. Caglioti, G. Rizzi, and F. Rossitto, Glide systems and Peierls stresses in FCC and BCC metals from phonon energies, *J. Appl. Phys.* **44**, 603 (1973).
 - [16] See Supplemental Material at <http://link.aps.org/supplemental/10.1103/PhysRevMaterials.6.L040601> for extended details of the finite element calculations.
 - [17] P. Ayres and P. Winchell, Dislocation arrangements resulting from the diffusion of Zn into Cu: Etch-pit studies, *J. Appl. Phys.* **39**, 4820 (1968).
 - [18] P. Ayres and P. Winchell, Dislocation arrangements resulting from the diffusion of Zn into Cu: Electron microscopy, *J. Appl. Phys.* **43**, 816 (1972).
 - [19] J. K. Boah and P. Winchell, Dislocation configurations developed during carburization of nickel, *Metall. Trans. A* **6**, 717 (1975).
 - [20] R. Mozzi and J. Lavine, Zn-diffusion-induced damage in InSb diodes, *J. Appl. Phys.* **41**, 280 (1970).
 - [21] I. M. Sukhodreva and L. D. Cheryukanova, Formation of dislocations in germanium during the diffusion of arsenic, *Fiz. Tverd. Tela* **10**, 932 (1968).
 - [22] G. Schwuttke and H. Queisser, X-ray observations of diffusion-induced dislocations in silicon, *J. Appl. Phys.* **33**, 1540 (1962).
 - [23] D. P. Miller, J. E. Moore, and C. Moore, Boron induced dislocations in silicon, *J. Appl. Phys.* **33**, 2648 (1962).
 - [24] J. Washburn, G. Thomas, and H. Queisser, Diffusion-induced dislocations in silicon, *J. Appl. Phys.* **35**, 1909 (1964).
 - [25] M. Armacanqui and R. Oriani, Plastic deformation in BCC alloys induced by hydrogen concentration gradients, *Mater. Sci. Eng.* **91**, 143 (1987).